APPLIED SCIENCES AND ENGINEERING

Detection and isolation of free cancer cells from ascites and peritoneal lavages using optically induced electrokinetics (OEK)

Yuzhao Zhang[1,2,3]*, Junhua Zhao[4,5]*, Haibo Yu[1,2†], Pan Li[1,2,3], Wenfeng Liang[6], Zhu Liu[1,2], Gwo-Bin Lee[7], Lianqing Liu[1,2], Wen Jung Li[1,2,8†], Zhenning Wang[4,5†]

Detection of free gastric cancer cells in peritoneal lavages and ascites plays a vital role in gastric cancer. However, due to the low content of cancer cells in patients' peritoneal lavages, traditional detection methods lack sensitivity and cannot satisfy clinical demand. In this study, we used an optically induced electrokinetics (OEK) microfluidic method for label-free separation and characterization of patient gastric cancer cells. This method showed high effectiveness and sensitivity. We successfully separated cancer cells from a simulated peritoneal lavage mixture of gastric cancer cell lines and peritoneal lavage cells in a ratio of 1:1000. We further separated gastric cancer cells from six patients' ascites with purity up to 71%. In addition, we measured the cell membrane capacitances, which may be used as a biomarker for gastric cancer cells. Thus, our method can be used to effectively and rapidly detect peritoneal metastasis and to acquire cellular electrical information.

INTRODUCTION

Gastric cancer is the fifth most frequently diagnosed cancer and the third leading cause of cancer death worldwide, accounting for more than 1 million new cases and nearly 800,000 deaths per year (*1*). Despite improvements in treatment, the prognosis for patients with gastric cancer is still unsatisfactory, especially for patients suffering from peritoneal metastasis (*2*–*4*). Implantation of free gastric cancer cells into the peritoneal cavity is believed to cause peritoneal metastasis, which is the most common route of tumor dissemination in gastric cancer (*3*, *5*). The poor prognosis of peritoneal metastasis is largely due to the difficulty in early diagnosis (*6*). Overall, the separation and characterization of cancer cells are essential for the early diagnosis of peritoneal metastasis. In clinical practice, cytological examinations of ascites and peritoneal lavages are performed to detect the free cancer cells in the peritoneal cavity. However, it is difficult for pathologists to distinguish gastric cancer cells from peritoneal mesothelial cells (the major components of ascites and peritoneal lavage). Like cancer cells, peritoneal mesothelial cells are epithelial in origin (*7*) and may show similar characteristics. Moreover, this conventional method also lacks sensitivity (*8*–*10*), as it is difficult to identify the few cancer cells among a large number of cells. In addition, cytological examination relies on cell staining, which is time-consuming and does not provide live cells for further use. At the same time, the similarity between cancer and mesothelial cells also limits the use of certain advanced methods such as CellSearch, which relies on epithelial makers to label and separate circulating cancer cells in blood samples (*11*). Therefore, there is an urgent need for a new label-free, time-saving, and diagnostic method that can distinguish and separate live gastric cancer cells with high sensitivity.

The establishment of new physical mechanisms has led to breakthroughs to cell separation in biomedical engineering. Microfluidics technologies are used to precisely control, manipulate, and analyze fluids through deliberately designed microchannels (*12*). Different shapes of microfluidic systems have been fabricated to purify blood cells, exosomes, and neutrophils (*13*–*16*). Other systems have been developed to separate red blood cells, white blood cells, and cancer cell lines (HepG2, SKBR3, A549, and BGC823) from blood samples (*17*, *18*). Despite the benefits of automatically and continuously separating cells, microfluidic systems require complicated designs and fabrication processes and lack interactive operation within the microfluidic chip. Therefore, integrating other controllable micro/nanomanipulation technologies within microfluidic systems is highly favorable for cell separation; this also reduces the demand of the microchannel design. For example, integrated systems of optical tweezers and microfluidic chips have been used for rapidly purifying mammalian cells, yeast cells, and human embryonic cells (*19*–*21*). The customized arrays of permanent magnets have been combined with microfluidics to separate white blood cells from whole human blood (*22*). Acoustic tweezer techniques have also been combined with microfluidics for separating alginate bead encapsulated cells (*23*), isolating MCF-7 cells from leukocytes (*24*), selecting exosomes from whole blood samples (*25*), isolating exosomes from saliva samples (*26*), and separating extracellular vesicles and lipoproteins (*27*). Furthermore, dielectrophoresis (DEP) integrated microfluidics have also been used to effectively separate cancer cell lines (NCI-60 and MCF-7) from leukocytes or red blood cells (*28*, *29*) and isolate bacterial cells from blood cells (*30*). The technology of integrating multiple systems on the microfluidic platform has also been reported; for example, integrating acoustophoresis and electroactive microwell array with microfluidics can separate circulating tumor cells and achieve single-cell trapping and imaging (*31*). There is no doubt that these techniques can be applied to cell separation with high

[1]State Key Laboratory of Robotics, Shenyang Institute of Automation, Chinese Academy of Sciences, Shenyang 110016, China. [2]Institutes for Robotics and Intelligent Manufacturing, Chinese Academy of Sciences, Shenyang 110169, China. [3]University of Chinese Academy of Sciences, Beijing 100049, China. [4]Department of Surgical Oncology and General Surgery, the First Hospital of China Medical University, Shenyang, China. [5]Key Laboratory of Precision Diagnosis and Treatment of Gastrointestinal Tumors, Ministry of Education, Shenyang, China. [6]School of Mechanical Engineering, Shenyang Jianzhu University, Shenyang 110168, China. [7]Department of Power Mechanical Engineering, National Tsing Hua University, Hsinchu, Taiwan. [8]Department of Mechanical Engineering, City University of Hong Kong, Hong Kong, China.
*These authors contributed equally to this work and should be considered co–first authors.
†Corresponding author. Email: josieon826@sina.cn (Z.W.); wenjli@cityu.edu.hk (W.J.L.); yuhaibo@sia.cn (H.Y.)

purification and recovery rates. However, optical tweezers need expensive laser equipment, which might cause photo damage and affect the cell activity; on the other hand, acoustic tweezers and DEP require predesigned physical electrodes that will increase system complexity while reducing the flexibility of the system and time. Ideally, the rapid separation of living cells and label-free extraction of intrinsic characteristics of samples are essential for early diagnosis of peritoneal metastasis in gastric cancer.

A label-free, nondestructive, and rapid optical-induced technique, called optoelectronic tweezers, was designed to manipulate nanoparticles and cells (*32*). In this system, a common projector projects digital light patterns onto a photoconductive layer to serve as a dynamic electrode for generating localized nonuniform electric fields. This is also recognized as optically induced dielectrophoresis (ODEP) or optically induced electrokinetics (OEK). Compared with traditional DEP techniques, optically induced techniques can produce dynamic light patterns in real time to act as virtual electrodes; there is no prefabrication requirement or replacement of rigid electrodes before or during the micro/nanomanipulation processes. Thus, the functions based on DEP can be realized along with real-time manipulations that can be performed during the separation. Moreover, the visible light illumination renders the optically induced technique with low radiation intensity, thereby facilitating noninvasive manipulation of biological samples. Optically induced techniques can isolate live and dead cells (*33*) and Raji cells from red blood cells (*34*); in addition, these techniques can integrate with microfluidics for manipulating cells and alginate microbeads (*35*), isolating cancer cell lines [prostate cancer cells (PC-3) and human oral cancer cells (OEC-M1)] and H209 cancer cell clusters from blood samples (*36*–*38*). Although intensive studies have been conducted using cell separation on the basis of optically induced techniques, few studies have focused on separation of cancer cells in complete clinical samples. It is unknown whether these techniques are able to separate cancer cells from normal epithelial cells. Furthermore, the prior experiments only focused on cell separation and characterization of separated cells was not performed. As mentioned above, both separation and characterization of gastric cancer cells play a crucial role in the early diagnosis of peritoneal metastasis.

In this study, we first applied the OEK method to achieve rapid separation of live gastric cancer cells from complete patients' ascites and label-free characterization of gastric cancer cells in a novel microfluidic chip, which could benefit diagnosis of peritoneal metastasis in gastric cancer. Both the polarization model of cells and the solution model of cell membrane capacitance were established for cell separation and characterization. The size, crossover frequencies, and cell membrane capacitances of ascites' gastric cancer cells, peritoneal lavage cells, and SGC-7901 cells were measured. Taking advantage of the difference in size and cell membrane capacitance between the gastric cancer cells and peritoneal lavage cells, we used the OEK method for cell separation. In addition, we designed a manual plastic microhose to extract the separated cells for cytological examinations. We successfully separated gastric cancer cells from patients' ascites and measured the cell membrane capacitances. The ascites samples were solely from clinical samples as opposed to cell mixture with cell lines. The cytological examinations conducted after cell collection revealed up to 71% purity. The experiments demonstrated that the proposed OEK method is capable of meeting the critical requirement for the clinical detection of peritoneal metastasis in gastric cancer. Furthermore, the cell membrane capacitance that was measured during separation can also be used as a biomarker, as part of cellular information.

RESULTS

OEK-based cancer cell characterization and separation

The main steps of the experimental process are outlined in Fig. 1. First, doctors collect patients' ascites during the cancer test or treatments. Collected ascites contain a large number of peritoneal mesothelial cells and few gastric cancer cells. The separation of gastric cancer cells and the acquisition of cell membrane capacitance can be achieved by placing ascites into microfluidic chips via OEK. The illustration of an OEK system is shown in Fig. 2A. In brief, the light pattern is generated by a computer, which is connected to a projector. The light pattern is focused on the bottom layer of the OEK microfluidic chip by the condenser lens, which is placed above the projector. The OEK microfluidic chip is placed on the three-dimensional (3D) motion stage, and the charge-coupled device (CCD) camera records the manipulation process within the chip. The signal generator is connected to the OEK microfluidic chip. A plastic hose connected to the syringe pump is placed into the OEK microfluidic chip for collecting the separated cells, as shown in Fig. 2B. The OEK microfluidic chip consists of three layers (Fig. 2C): the top glass coated with indium tin oxide film (ITO glass), the double-adhesive tape fabricated with the microfluidic channel, and hydrogenated amorphous silicon (a-Si:H) deposited onto the ITO glass layer (see method and fig. S1). When the dynamic light pattern generated by the computer is projected onto the a-Si:H layer, the conductivity of the illuminated area will increase due to the photogeneration of electron hole pairs. This allows the dynamic light pattern to act as electrodes. Subsequently, the AC signal is applied on the top and bottom of the ITO glass to generate nonuniform electric fields in the solution. Within the electric field, the cells in the solution are electrically polarized and when the frequency of the applied AC voltage is in the range of 7 to 500 kHz, the cells are mainly manipulated by DEP force in the solution (*34*). Thus, we can manipulate cells in the OEK chip by the dynamic light patterns.

Identification of cell electrical parameters and analysis of cell separation

In this study, DEP force is applied across the cells in the solution in an OEK microfluidic chip. In a simplified model, cells are spherical particles and can be modeled as a single layer of shell core, as shown in Fig. 3A. Details of the cell polarization model are shown in Materials and Methods. When the cells are subjected to DEP force in the solution, it will be attracted and repelled by the light pattern in two distinguishable states. As the frequency of the applied AC voltage increases, the cells will move from the "repulsion" state to the "attraction" state. That is, cells that are under negative DEP force are in a "repulsive" state and are repelled from the light pattern. Otherwise, they are under positive DEP force and are attracted toward the light pattern. The frequency at which the state of cell is changing from the repulsive state to the "attractive" state is defined as the crossover frequency (fig. S2). According to the cell polarization model, the crossover frequencies between different cells vary due to the differences of the cells' sizes and membrane capacitances. Consequently, cells of different sizes and membrane capacitances can be separated by using different crossover frequencies. Therefore, the cell membrane capacitance can be identified through the parameters of size and crossover frequency in the experiments.

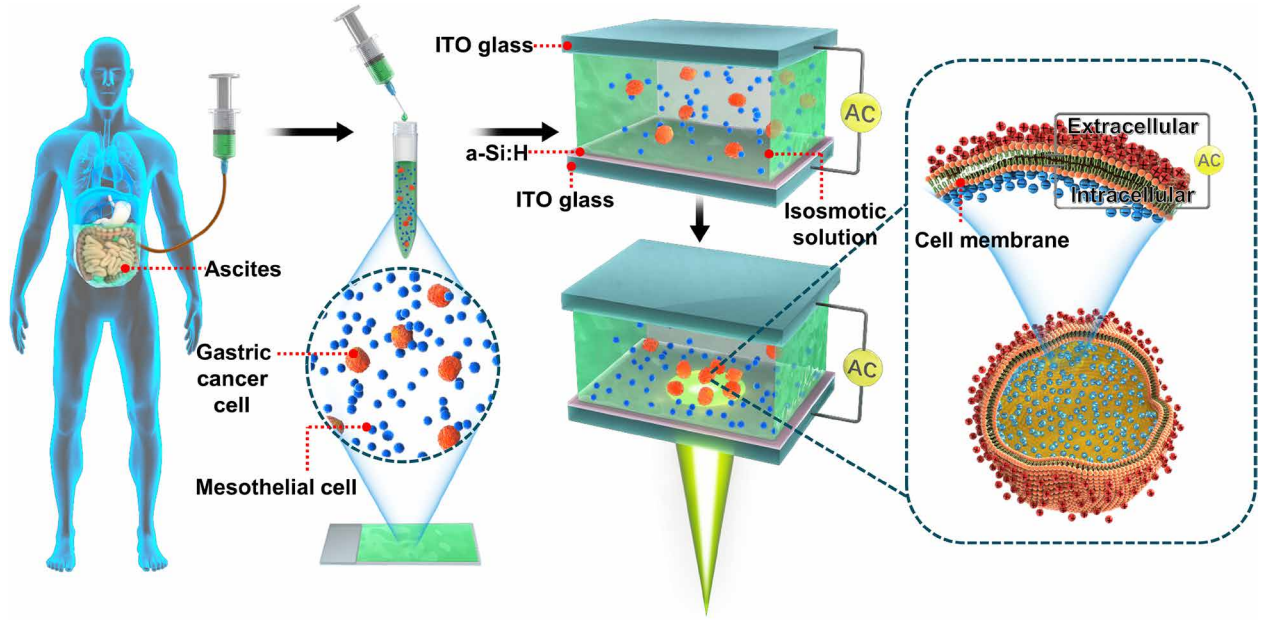

Fig. 1. OEK microfluidic chip developed for detecting peritoneal metastasis and cell membrane capacitance. Ascites obtained from patients are placed in the OEK microfluidic chip. The gastric cancer cells can be separated from ascites rapidly and label-free. Meanwhile, the cell membrane capacitance of the separated cells is obtained.

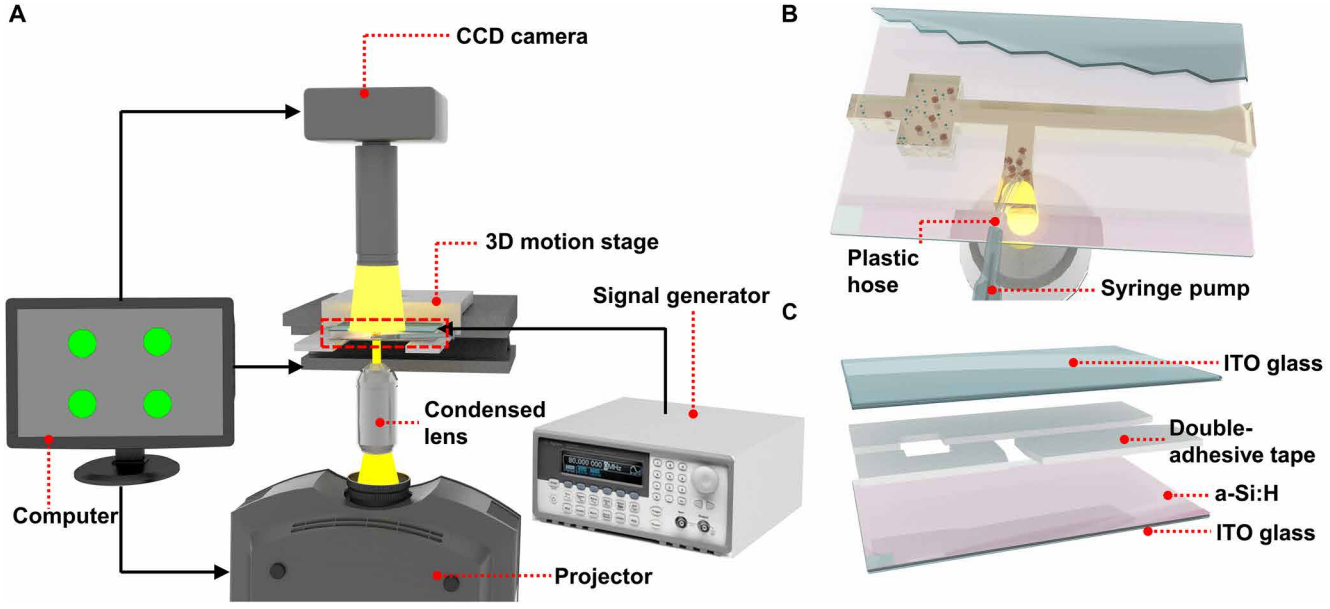

Fig. 2. Experimental system and the OEK microfluidic chip. (**A**) Schematic diagram of the OEK system. The system consists of a computer, a projector, a condensed lens, a signal generator, a three-dimensional (3D) motion stage, a charge-coupled device (CCD) camera, and the OEK microfluidic chip. (**B**) Schematic of extraction device. The plastic hose, which is connected to the syringe pump, is used for collecting separated cells. (**C**) Structure of the OEK microfluidic chip. The chip consists of three parts: glass coated with indium tin oxide film (ITO glass), double-adhesive tape, which is used for fabrication of the microchannel, and coated hydrogenated amorphous silicon (a-Si:H) ITO glass.

Four types of cells were analyzed: SGC-7901 cell line cancer cells and three hysteromyoma lavage samples, which were mainly composed of peritoneal mesothelial cells without cancer cells (patients M1, M2, and M3). Before use for the experiments, the expressions of tumor marker MOC-31 were measured for peritoneal lavage samples. The results showed that none of the samples expressed MOC-31 (fig. S3). Figure 3B shows the radii of these cells, which were 8.3 ± 1.03 μm, 3.63 ± 0.27 μm, 3.39 ± 0.25 μm, and 4.27 ± 0.75 μm, respectively. In an isosmotic solution with a liquid conductivity of approximately 70 μs/cm, the crossover frequency of each cell was measured in Fig. 3C. The results were 22.97 ± 4.24 kHz for SGC-7901 and 142.8 ± 37.03 kHz, 156.68 ± 50.9 kHz, and 109.22 ± 28.95 kHz

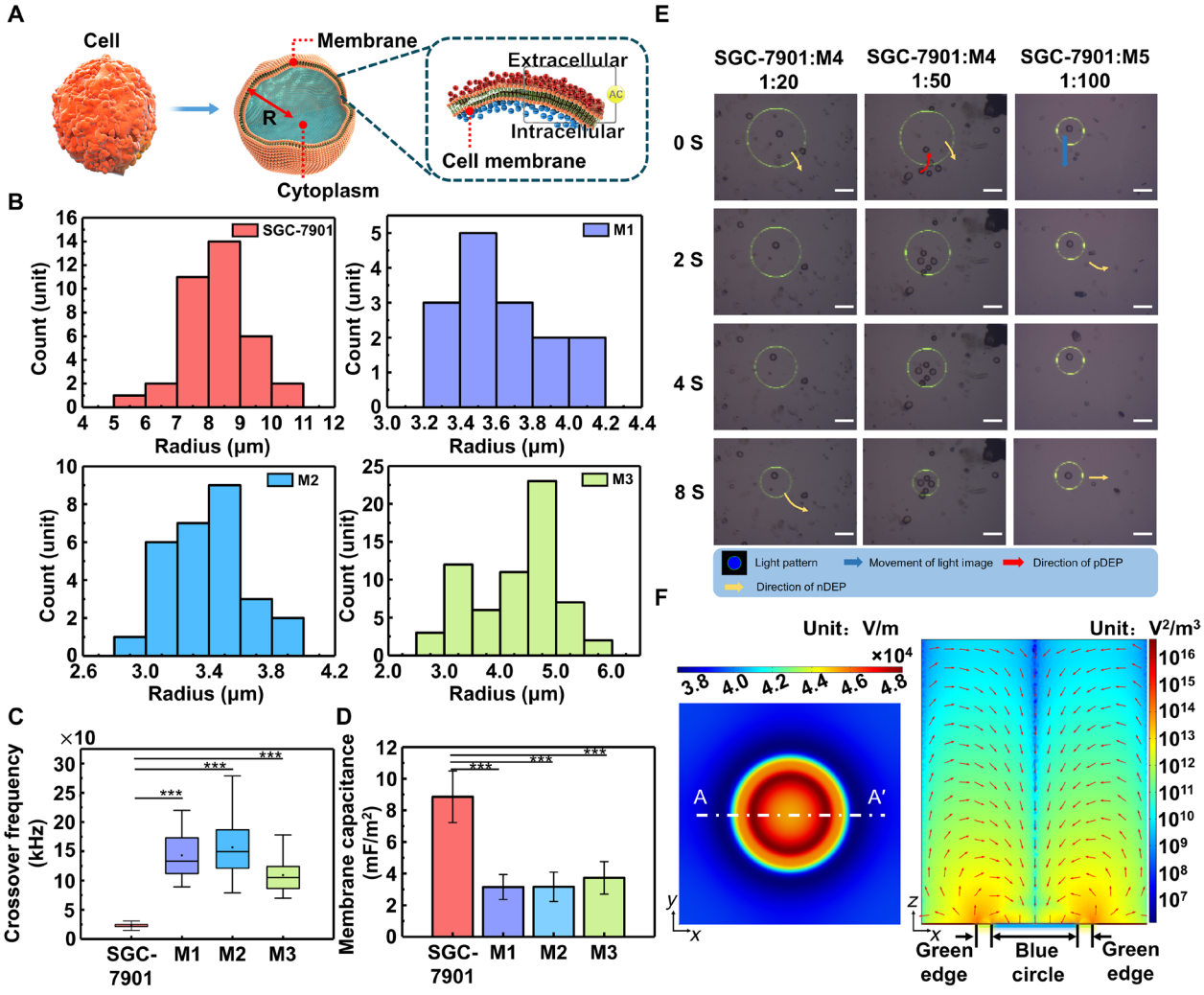

Fig. 3. Cell polarization model and cell separation. (**A**) A single layer of shell core model for cells is established in this system. The model is applied to the theoretical basis of cell separation and to the solution of cell membrane capacitance. (**B**) Radii of SGC-7901 cancer cell line cells and patients' peritoneal lavage cells (M1, M2, and M3). (**C**) Different crossover frequencies between SGC-7901 and patients' peritoneal lavage cells. ***$P < 0.001$. (**D**) Cell membrane capacitances of SGC-7901 and patients' peritoneal lavage cells. (**E**) Cell separation after mixing SGC-7901 with different patients' peritoneal lavage cells (M4 and M5) in a ratio of 1:20, 1:50, and 1:100. The AC voltage of 70 KHz 10 Vpp are applied on the OEK microfluidic chip in the illuminated area and some cells are applied by positive dielectrophoresis (pDEP) force and others are moving away from the light pattern by negative dielectrophoresis (nDEP) force. Scale bars, 50 μm. (**F**) The finite element method for numerical analysis results of electric field magnitudes $|E|$ and the direction of the ∇E^2 distribution.

for M1, M2, and M3 patient's peritoneal lavage cells, respectively. According to Eq. 4, the cell membrane capacitance of each cell type is calculated: 8.86 ± 1.63 mF/m^2 (n = 36) for SGC-7901, 3.15 ± 0.79 mF/m^2 (n = 15) for patient M1, 3.17 ± 0.93 mF/m^2 (n = 28) for patient M2, and 3.73 ± 1.03 mF/m^2 (n = 64) for patient M3, as shown in Fig. 3D.

Using the different crossover frequencies between the SGC-7901 cancer cells and peritoneal lavage cells, the two types of cells can be separated with frequencies from 30 to 80 kHz, with a liquid conductivity of approximately 70 μs/cm. Next, SGC-7901 cells were mixed with patient M4's peritoneal lavage cells in ratios of 1:20 and 1:50. SGC-7901 cells were mixed with patient M5's peritoneal lavage cells at a ratio of 1:100. The light pattern is a circle, which is filled with blue and the edge of the circle is green. In the ratio of 1:20 and 1:50, the radii changed from 70 to 35 μm. The radius of the light pattern was approximately 35 μm in the ratio of 1:100 and the moving speed of the circle was 0.5 mm at every step (see fig. S4). In Fig. 3E, the AC voltage of 10 Vpp (peak-to-peak value) with a frequency of 70 kHz was applied on the OEK microfluidic chip. Cells were visualized moving into the light pattern owing to the positive DEP force, while others moved away from the light pattern by negative DEP force. According to the previous crossover frequency experiments, the cells subjected to positive DEP were SGC-7901 cells and the other cells were peritoneal lavage cells. This provided a basis for the next step of cell separation and collection.

To verify the direction of positive and negative DEP forces applied to the cells, the finite element method for numerical analysis that resulted from electric field magnitudes $|E|$ and the direction of the ∇E^2 distribution are shown in Fig. 3F. In Fig. 3F, the left panel shows the electric field magnitudes on the a-Si:H surface. The

variations of the electric field magnitudes are larger on the edge of the light pattern, which is the junction of light and shade. The right figure is the cross-sectional distribution of AA′ (a line in Fig. 3F) of the direction of ∇E^2. The red arrows represent the direction of ∇E^2, which indicates the direction of positive DEP force. When positive DEP force is applied on the cells, they move into the light pattern and vice versa with negative DEP force. Thus, this simulation supports the possibility of using this type of light pattern; the simulation results also agree with our experiments processed in Fig. 3E.

Separation and collection of gastric cancer cells in the OEK microfluidic chip in 5 min

To further prove that our method can effectively separate gastric cancer cells from peritoneal lavage cells, we fabricated the OEK microfluidic chip to separate and collect gastric cancer cells. The details of fabrication are shown in Materials and Methods and supplementary figures. We fabricated a plastic hose with an outer diameter in the front section of approximately 100 to 200 μm, which allowed the front end of the plastic hose to enter the OEK microfluidic chip. Next, a T-type microchannel on the double-edged type was manufactured. The width of the main microchannel was 1 mm, the side microchannel was 0.5 mm, and the distance between the cell collection area and side microchannel was 2.5 mm. Before the chip was packaged, the surface of the coated a-Si:H ITO glass was treated with oxygen plasma to make the surface hydrophilic. A hydrophilic surface allows solutions to flow smoothly into the microchannel. Cell mixtures can be injected from the inlet and sucrose solution is injected into the side microchannel by the plastic hose. When the solution in the channel remains stable, the cells remain in the cell collection area. Exposure to light patterns in the cell collection area causes the gastric cancer cells to move into the light pattern by positive DEP force while the peritoneal lavage cells move away from the light pattern through negative DEP force. This can be manipulated by dragging the light pattern at the appropriate speed, which moves the separated cells to the side microchannel. When the separated cells are next to the plastic hose, the signal generator is turned off and the separated cells are extracted by syringe pump, as shown in Fig. 4A. After putting the prepared cell mixture into the microfluidic chip, the entire process of cell separation and collection in the OEK microfluidic chip can be completed in 5 min (see movie S1).

High sensitivity in cancer cell separation

As mentioned in Introduction, a diagnostic method or system that is able to separate cancer cells from ascites and lavage cells will provide a qualitative leap in peritoneal metastasis diagnosis. Therefore, to imitate ascites and gastric cancer lavage cells and verify whether our system could separate gastric cancer cells from large amounts of peritoneal lavage cells, we mixed gastric cancer cell line (SGC-7901 cells) with the peritoneal lavage cells in different ratios. Ratios of cancer cells:peritoneal lavage cells at 1:10, 1:100, and 1:1000 were used. Before mixing, the cancer cells were incubated with CellTracker Green 5-Chloromethylfluorescein Diacetate (CMFDA). The labeled and mixed cells were placed in the isosmotic solution and 10 Vpp AC voltage was applied at 60 kHz in the ratio of 1:10; 70 kHz was used in the ratios of 1:100 and 1:1000. The separated cells were extracted by the plastic hose and coated onto a glass slide. The cellular fluorescence of the cancer cells was imaged by a fluorescence microscope using a 10× objective, as shown in Fig. 4B. The red arrows show cells with green fluorescence, which indicated cancer cells. Following fluorescent imaging, the separated cells were stained by the Wright-Giemsa method. Figure 4B shows representative images of separated cells after separation. The cells were hyperchromatic with large nuclei, which conforms to the characteristics of cancer cells. The cell morphology of Wright-Giemsa–stained SGC-7901 cells was used for contrast (fig. S5). To summarize, in the 1:10 cell ratio, we found six cells under the microscope with five cells identified as cancer cells. For the 1:100 ratio, we found three cells, with all of them identified as cancer cells. In the 1:1000 ratio, we found five cells, with three cells identified as cancer cells. Figure 4B also shows the Wright-Giemsa–stained cell mixtures before separation. Moreover, to further verify our system, we incubated peritoneal lavage cells with CellTracker Red CMPTX and performed another cancer cell isolation as described above. Cancer cells were also incubated with CellTrack Green CMFDA, and the ratio of cancer cells:peritoneal lavage cells at 1:500 was used. Figure S6 (A and C) shows cellular fluorescence and Wright-Giemsa stain of cell mixture before separation. The labeled and mixed cells were placed in the isosmotic solution, and 10 Vpp AC voltage was applied at 70 kHz. The separated cells were with green fluorescence (as shown in the fluorescent image in fig. S6B) and hyperchromatic with large nuclei by Wright-Giemsa stain (fig. S6D), which conforms to the characteristics of cancer cells. In total, we found three cells, with two of them identified as cancer cells. In the 1:100 to 1:1000 ratios, it was challenging to find the cancer cells under a microscope without using the separation method. Compared to the traditional methods with low sensitivity, our methods successfully identified the cancer cells in the ratio of 1:100 and 1:1000.

Considering ascites not only have mesothelial cells and potential cancer cells but also have leukocytes, we collected leukocytes from blood samples after performing red blood cell lysis. Then, we measured the DEP force direction of leukocytes at 10 Vpp AC voltage and 70 kHz, which we used for isolating cancer cells from peritoneal lavage cells. As shown in fig. S7A, the results indicate that leukocytes were subjected to negative DEP force (as for peritoneal lavage cells) rather than positive DEP force as for the case of SGC-7901 cells. Moreover, we mixed SGC-7901 cells with the leukocytes. The ratio of cancer cells:leukocytes at 1:100 was used. Before mixing, the cancer cells were also incubated with CellTracker Green CMFDA. The mixed cells were placed in the isosmotic solution, and 10 Vpp AC voltage was applied at 70 kHz. The separated cells were with green fluorescence by fluorescent imaging (fig. S7B) and hyperchromatic with large nuclei by Wright-Giemsa stain (fig. S7C), which conforms to the characteristics of cancer cells. In total, we found four cells, with three of them identified as cancer cells. Figure S7D shows the Wright-Giemsa–stained cell mixtures before separation.

Separation and characterization of gastric cancer cells in patients' ascites

To further the studies, we applied the OEK method to clinical samples. To the best of our knowledge, the present study is the first to use this method to separate cancer cells in pure clinical samples. Patient samples A1, A2, and A3 are the ascites from patients who did not have any prior treatments. Samples A4 and A5 are from patients who had prior treatment, as shown in table S1. Similarly, the liquid conductivity and parameters on applied separated AC voltage are also shown in table S1. The radii and cell membrane capacitance of these separated cells were calculated. As shown in Fig. 5 (A and B), the radii are 7.64 ± 0.95 μm for A1, 6.63 ± 1.33 μm for A2, 7.72 ± 1.07 μm for A3, 6.44 ± 0.91 μm for A4, and 4.18 ± 0.98 μm

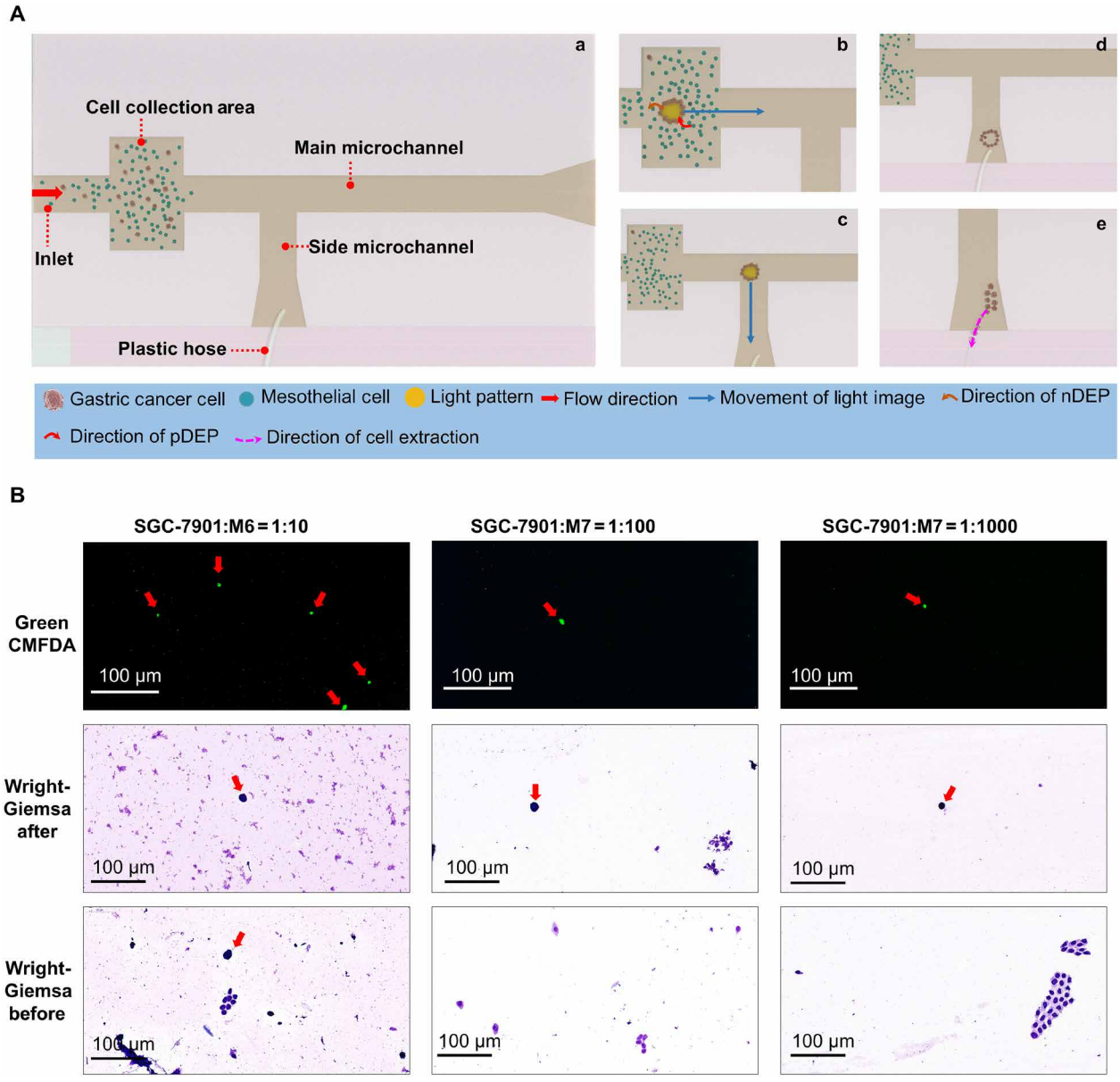

Fig. 4. Process of cell separation and identification of separated cells. (**A**) Process of cell separation in the OEK microfluidic chip. (a) and (b) show the process of cell separation in the cell mixture. (c) and (d) show the process of dragging separated cells next to the plastic hose in the OEK microfluidic chip. (e) shows separated cells collected by the plastic hose. (**B**) Cell separation and identification of simulated peritoneal lavage. We mixed SGC-7901 cells, which were incubated with CellTracker Green CMFDA with peritoneal lavage cells in different ratios: 1:10, 1:100, and 1:1000. The separated cells were imaged by a fluorescence microscope using a 10× objective. The second panel of (B) shows representative cells after separation stained with Wright-Giemsa. The cells were hyperchromatic with large nuclei, conforming to the characteristics of cancer cells. The third panel of (B) shows the cells before separation stained with Wright-Giemsa. The red arrows in (B) point to gastric cancer cells.

for A5. The corresponding cell membrane capacitances are 6.95 ± 2.05 mF/m^2 (n = 18), 5.33 ± 1.62 mF/m^2 (n = 65), 5.05 ± 1.21 mF/m^2 (n = 23), 12.20 ± 2.67 mF/m^2 (n = 29), and 7.79 ± 1.69 mF/m^2 (n = 67). Figure 5C shows the processes of cell separation in the OEK microfluidic chip. Last, cytological examination on the separated cells was performed. Figure 5D shows representative images of stained separated cells after separation and ascites cells before separation. The separated cells were hyperchromatic with large nuclei, which conformed to the characteristics of cancer cells as identified by a pathologist. The total cell number results are shown in table S1.

Separation and characterization of gastric cancer cells from different stages of one patient

The studies above confirmed that our system is capable of separating cancer cells from ascites in a single step. To verify that our system works perfectly during the entire process, we applied our system to different stages of ascites from one patient (patient A6). In total,

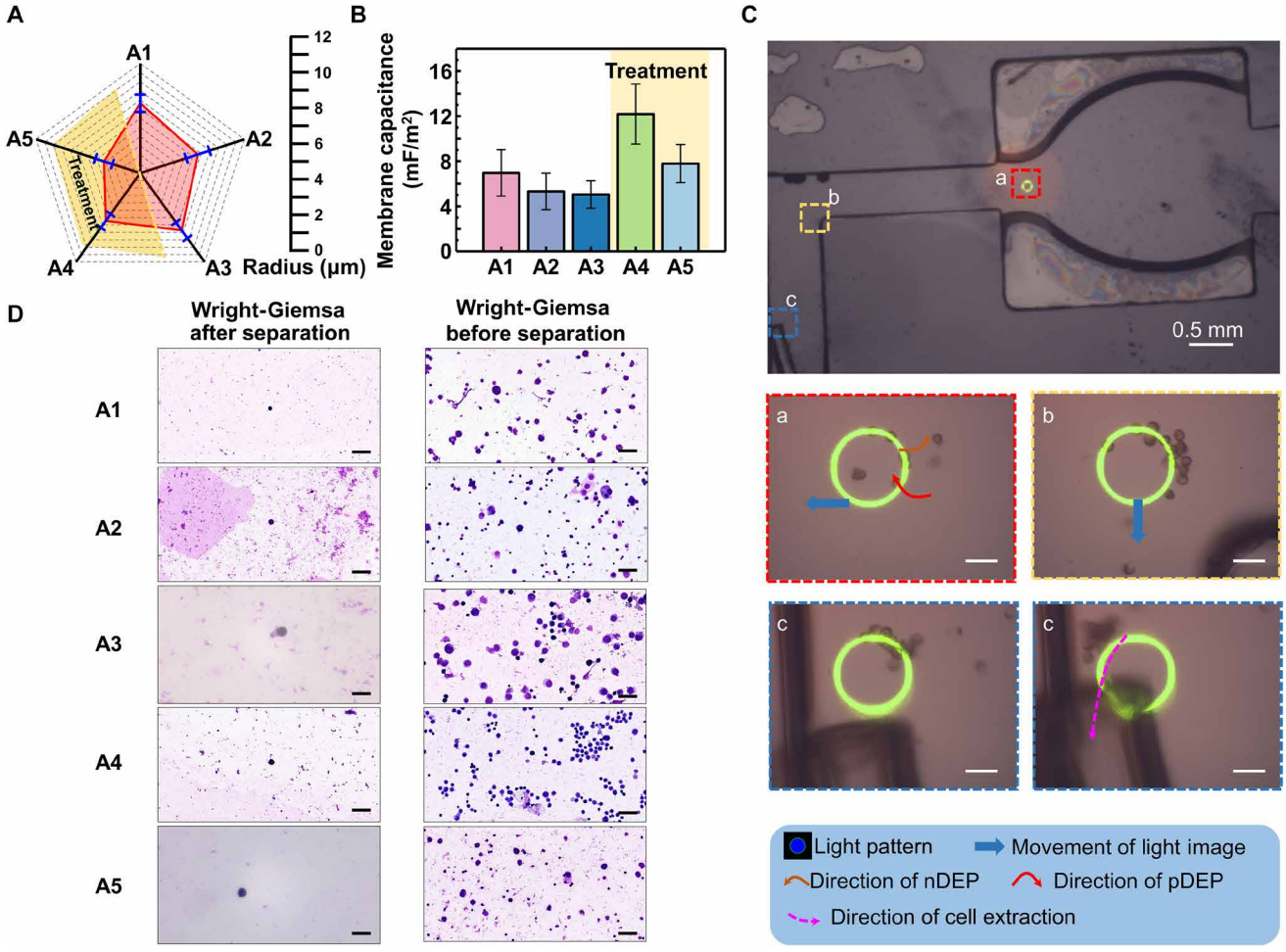

Fig. 5. Cell separation of patients' ascites. We separated gastric cancer cells from patients' ascites (A1 to A5) with appropriate external frequencies. A1, A2, and A3 are patients' ascites before treatment and A4 and A5 are after treatment. (**A**) Radii of separated cells. (**B**) Cell membrane capacitances of separated cells. (**C**) Process of cell separation in the OEK microfluidic chip. (a) demonstrates separating gastric cancer cells in the cell collection area. (b) is the process of opt dragging separated cells to the plastic hose. (c) shows the collection process by plastic hose. Scale bars, 50 μm. (**D**) Wright-Giemsa staining of cells. The left panel shows representative cells after separation. The cells were hyperchromatic with large nuclei, conforming to the characteristics of cancer cells. The right panel shows the cells before separation. Scale bars, 50 μm.

three stages of ascites were collected from patient A6. The first stage of ascites (A6-1) was collected before the patient receives any treatment. The second (A6-2) and third (A6-3) stage were collected at different time points after the patient received treatment. Concrete information of the patient and treatment are shown in table S1. The separated parameters of applied AC voltage and liquid conductivity are also shown in table S1. The radius and crossover frequency of each cell was calculated to obtain the cell membrane capacitance. The average radii of cells are 5.8 ± 1.3 μm for A6-1, 5.35 ± 1.01 μm for A6-2, and 5.19 ± 2.34 μm for A6-3, as shown in Fig. 6A. Thus, the cell membrane capacitances are 6.24 ± 2.41 mF/m^2 (n = 39) for A6-1, 7.63 ± 2.39 mF/m^2 (n = 51) for A6-2, and 8.01 ± 2.15 mF/m^2 (n = 38) for A6-3. As shown in Fig. 6B, the cell membrane capacitances show an upward trend as treatment progresses. Next, a 10 Vpp AC voltage was applied with frequencies of 60 to 80 kHz to separate the A6 patient's different stages' ascites. Figure 6B shows the Wright-Giemsa staining of ascites cells before separation and separated cells after separation. The cells were hyperchromatic with a large nucleus, as we previously observed. To summarize, for A6-1 ascites, we found 11 cells with 8 cells identified as cancer cells. For A6-2 ascites, we found 20 cells under the microscope with 14 cells identified as cancer cells. For A6-3 ascites, we found 6 cells under the microscope with 5 cells identified as cancer cells.

To further validate our results, we performed another separation for the ascites samples (A2, A3, A4, and A6-3). We validated the isolated cancer cells using epithelial tumor marker EpCAM (epithelial cell adhesion molecule) by the immunofluorescence method. The results showed that EpCAM was positively expressed in the isolated cells from these samples (Fig. 6D).

Summary of cell membrane capacitances and purity

All of the cell membrane capacitances (Fig. 6E) were compared together through analysis of variance (ANOVA) with Bonferroni method. The cell membrane capacitances of the eight ascites (A1 to A5 and A6-1 to A6-3) separated cells were all significantly higher than those of three (M1 to M3) peritoneal lavage cells (all $P < 0.01$). Moreover, the cell membrane capacitances of separated cells from A5, A6-2, and A6-3 were similar to that of SGC-7901 cells ($P = 0.36$,

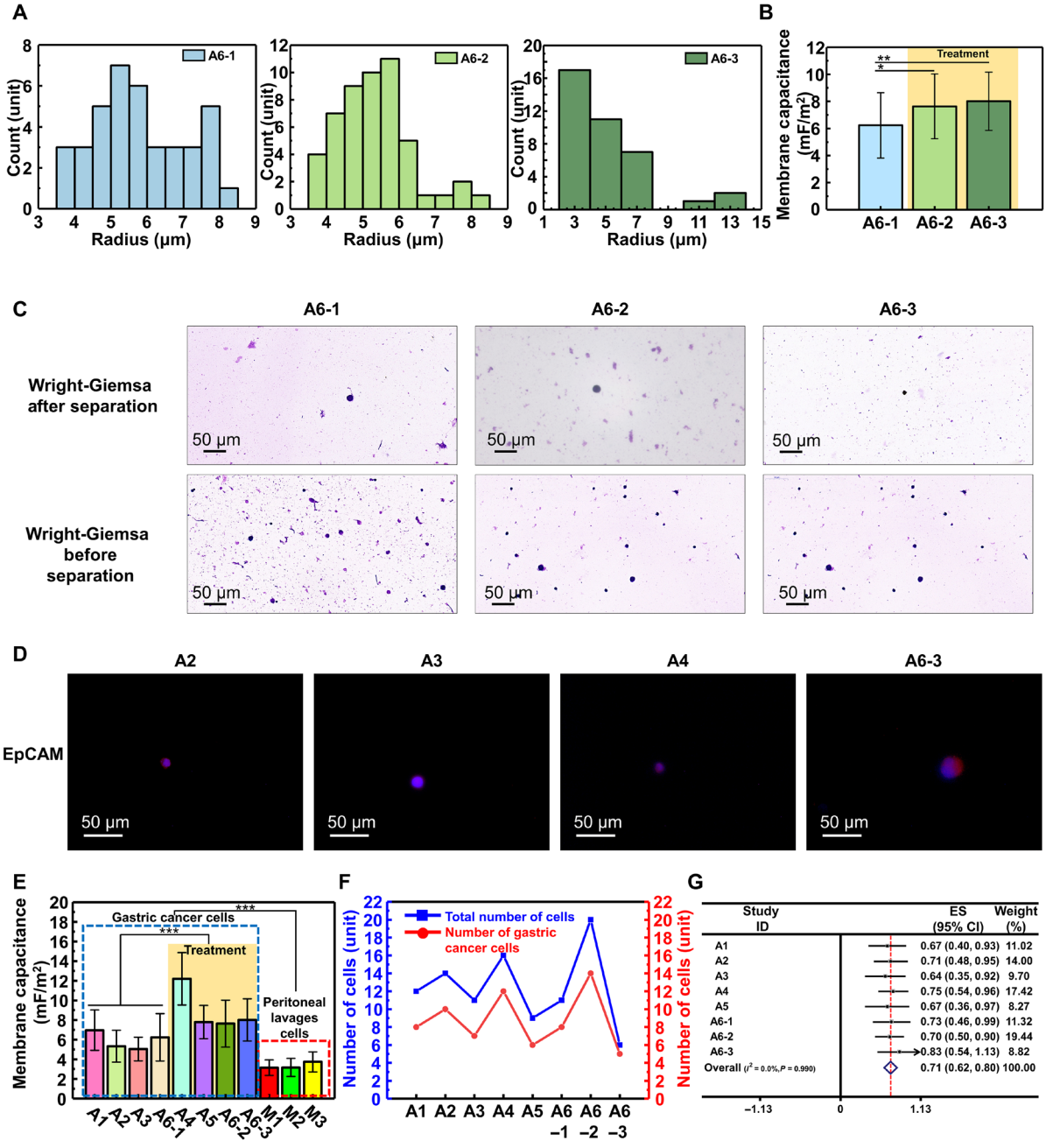

Fig. 6. Cell separation in different stages of patient A6 and results summary. We separated patient A6's ascites in the different stages; A6-1 is the ascites before the treatment, and A6-2 and A6-3 are the ascites after treatment. (**A**) Radii of separated cells in the different stages. (**B**) Cell membrane capacitances of separated cells. (**C**) Wright-Giemsa staining of cells. The first panel shows the representative cells after separation. The cells were hyperchromatic with large nuclei, conforming to the characteristics of cancer cells. The second panel shows the cells before separation. Scale bars, 50 μm. (**D**) EpCAM was positively expressed in the isolated cells from sample A2, A3, A4, and A6-3. (**E**) Cell membrane capacitance summary of clinical samples. The cell membrane capacitances of the ascites separated cells were all significantly higher than that of three peritoneal lavage cells. Separated cells' membrane capacitances from ascites after treatment are higher than those before treatment. (**F**) Purity statistics of cell separations in eight ascites samples. (**G**) The overall purity of the cell separation. This overall purity was calculated through pooled analysis by Stata. The purity was 71% [95% confidence interval (CI), 62 to 80%]. **P* < 0.05. ***P* < 0.01. ****P* < 0.001.

0.16, and 1.00 for A5, A6-2, and A6-3, separately). These results further indicate that the separated cells showed distinguishing characteristics that separate them from peritoneal lavage cells and indicate similar characteristics to gastric cancer cells. For all eight ascites samples, four were collected before the patient received any treatment (A1, A2, A3, and A6-1) and the other four samples were collected after treatment (A4, A5, A6-2, and A6-3). Separated cells' membrane capacitances from ascites after treatment are higher than those before treatment ($P < 0.01$). The increase in cell membrane capacitance could be attributed to the thickness of cell membrane, which will be addressed in future studies. We also measured the cell membrane capacitance of SGC-7901 cells by patch clamp. The results of patch

clamp showed that the cell membrane capacitances of SGC-7901 were 15.41 ± 2.47 pF (n = 12, fig. S8). Furthermore, we analyzed the overall purity of the of the cell separation from ascites through pooled analysis by Stata software. As shown in Fig. 6 (F and G), the overall purity was 71%.

DISCUSSION

Early diagnosis for peritoneal metastasis diagnosis is vital to enhancing the prognosis of patients with gastric cancer. It is a very challenging task to separate and identify cancer cells from ascites and peritoneal lavages. The sensitivity of conventional cytological examinations has been limited by the difficulty of distinguishing a small number of cancer cells from a larger number of noncancer cells (*8*–*10*). Molecular detection methods (*39*) lack a uniform definition of positive status, thus limiting its wide clinical use.

In this study, we introduced a new method on the basis of OEK for the diagnosis of peritoneal metastasis. This method has the ability to separate and characterize cancer cells from ascites and lavage cells with the advantages of speed, simplicity, and being label-free. Moreover, this is the first time that the OEK method was successfully applied to the separation of clinical gastric cancer ascites samples. Furthermore, this method also successfully characterized the electrical properties of the separated cells to obtain their membrane capacitances.

To verify our system in cancer cell separations from ascites and peritoneal lavages, we designed progressive and methodical experiments. First, under the liquid conductivity of 70 μs/cm, the crossover frequency of gastric cancer cells and hysteromyoma lavage cells was measured. Peritoneal lavage cells from patients with hysteromyoma were used for cell characteristic measurements and as background cells in cell mixtures. Peritoneal lavage cells were mainly composed of peritoneal mesothelial cells and, importantly, free of cancer cells. Our results showed that the cell membrane capacitances and radii of gastric cancer cells were significantly lower compared to peritoneal lavage cells, which provided a theoretical basis for cell separation. To imitate ascites and gastric cancer lavage cells, gastric cancer cells from cell lines were mixed with peritoneal lavage cells in different ratios. The ratios of 1:10, 1:20, and 1:50 were similar to the ratio of cancer cells to peritoneal lavage cells in ascites. The ratios of 1:100 and 1:1000 were similar to the peritoneal lavage fluid from patients with gastric cancer. The results showed that our system is able to separate out the cancer cell even at a ratio of 1:1000, which proved a higher sensitivity than traditional methods. This lays a solid foundation for the future usage of this system in separating clinical ascites samples. In total, we tested eight different ascites cells from six patients with different treatment backgrounds; the purity of 71% was calculated through pooled analysis by Stata (see fig. S5). Patients A1, A2, A3, and A6-1 had not received relevant treatment before the ascites were collected. Patients A4, A5, A6-2, and A6-3 suffered from recurrent gastric cancer and had received surgery with adjuvant chemotherapy before the ascites were collected. Ascites were collected at three different stages from patient A6. Thus, our system is suitable for ascites cells from different patients and treatment histories, which demonstrates a bright prospect for the wide clinical usage of this system in the future. In addition, the number of separated cells obtained in the latter part of the study was relatively higher than that in the earlier part of the study. This may be due to the greater number of preseparation ascites cells than preseparation lavage cells. In addition, in the latter part of the study, the research team had accumulated more experience and skill with these techniques.

To verify the effectiveness of our method, we performed cytological examination to confirm the separation of cancer cells. As Papanicolaou stain is now widely adopted in the clinic (*6*, *39*, *40*), we first used this method. However, in the Papanicolaou stain procedure, one slide goes through multiple procedural steps, which could lead to cell loss. Thus, this method was not suitable for our study due to the low cell number. Although the Wright-Giemsa stain is traditionally used for blood cell staining, the stain shows the characteristics of cancer cells and is able to distinguish cancer cells from peritoneal mesothelial cells. Furthermore, there is less cell loss during the Wright-Giemsa procedure. The Wright-Giemsa stain proved that our system could separate cancer cells from all eight ascites samples. Moreover, most of the separated cells were identified as cancer cells with a pooled purity of 71%. The separated cells did include some noncancer cells, which were mainly peritoneal mesothelial cells. We postulate that this is due to the fact that when cancer cells were subjected to positive DEP force, peritoneal lavage cells inevitably mix in due to the complex movement between cells. This can be solved by using a more complex dynamic light pattern. EpCAM is an established diagnostic biomarker for epithelial malignancies (*41*). We found that EpCAM was positively expressed in isolated cells, which further proved that the isolated cells were cancer cells. As the purity of our method was up to 71% and showed the potential to enrich cancer cells, combining our methods with EpCAM expression assay may have a good prospect in improving the diagnostic sensitivity of peritoneal metastasis.

We have also shown that cell membrane capacitances could be used as a biomarker of the intrinsic electrical characteristics of gastric cancer cells and peritoneal lavage cells. The gastric cancer cell line showed a significantly higher cell membrane capacitance in comparison with peritoneal lavage cells from three different patients. This difference may help to explain why our system could separate out cancer cells in ascites and imitative lavage cells. Afterward, we used the same method to measure cell membrane capacitances of the cells separated from ascites. These separated cells showed similar cell membrane capacitances to the gastric cancer cell line, which reflected on the accuracy of the separation. Although the reason for the difference in cell membrane capacitance needs to be further studied in follow-up research, it is plausible that cell membrane capacitance can be used as a biomarker, which can be part of cellular multidimensional information. To verify our method, we also measured the cell membrane capacitance of SGC-7901 cells by patch clamp. The results of patch clamp showed that the cell membrane capacitances of SGC-7901 were 15.41 ± 2.47 pF (n = 12, fig. S8 in the revised manuscript). We should note here that a more precise terminology to use to describe our reported results in the manuscript should be "cell membrane capacitance/unit area." Therefore, to compare our results to results obtained from the patch clamp, the following relationship should be used

$$C_c = S_c * C_{mem}$$

where C_c is the cell membrane capacitance (as measured by the patch clamp), S_c is the cell surface area, and C_{mem} is the cell membrane capacitance per unit area (as measured by the OEK method). Therefore, on the basis of the average C_{mem} value (8.86 mF/m^2) measured by our OEK method, the estimated surface area of an SGC-7901 cell is

about 1739.2 μm^2. If we treat cells as spheres with smooth membrane surface (i.e., sphere with a surface area of $4\pi R^2$, where R is the radius of a sphere), the cell radius calculated from our method is about 11.8 μm. However, note that the surface area of cells is affected by multiple factors (*42*), especially that the cell membrane infoldings may increase the total cell surface area and make the value higher than $4\pi R^2$ (*43*–*45*). Thus, it is reasonable that the value 11.8 μm was higher than the average measured value of 8.3 μm (i.e., radius of cells measured by optical microscope). Thus, the cell membrane capacitance measured by our method is in accordance with the value measured by the patch clamp technique.

In summary, we demonstrated that the OEK method could rapidly and freely label separate live gastric cancer cells from patients' ascites for diagnosis of peritoneal metastasis in gastric cancer; it could also reveal the electrical characteristics of gastric cancer cells at the same time. The collection of live gastric cancer cells allows us to measure cellular multidimensional information, such as the measurement of cell softness and hardness by combining with atomic force microscopy, and investigate the causes of changes in cell membrane capacitances. Furthermore, the direct separation of living cancer cells from clinical samples is of great significance to clinical medicine. To the best of our knowledge, our study is the first to achieve the separation of living gastric cancer cells from ascites. In the future, separated live cancer cells could be further cultured and used to study the mechanism of peritoneal metastasis. Moreover, we could perform cancer cell sequencing and acquire new information about peritoneal metastasis.

MATERIALS AND METHODS

Experimental system

The experimental system is shown in Fig. 2A. The OEK microfluidic chip was placed on the 3D motion stage (Leetro AutoMation Co. Ltd., China). The light pattern was drawn on the commercial graphics software package (Flash 11, Adobe, USA) and projected by an LCD projector (VPL-F400X, Sony, Japan) and then focused on the a-Si:H substrate via a condenser objective (Nikon, MS plan, ×50). A functional generator (Agilent 33522A, USA) was connected to the top and bottom ITO glasses of the OEK microfluidic chip and AC voltage was applied. All of the separation and collection processes were observed and recorded via a CCD camera (DH-SV1411FC, DaHeng Image, China), which was connected to a computer.

OEK microfluidic chip

The structure of the OEK structure is shown in Fig. 2 (B and C). The 185-nm ITO film was coated on a 1.1-mm-thick glass by magnetron sputtering. The bottom layer was prepared by plasma-enhanced chemical vapor deposition technology. A 1-μm a-Si:H was coated on the ITO glass. The microfluidic channel was made on the double-edged adhesive type (VHB/300LSE, 3 M China, China). The microchannel was fabricated by a layer engraving machine (FL-570, Hengchunyuan Machinery Equipment, China) first and manual secondary processing. The plastic hose was made using a plastic dispensing dropper. The front end of the dropper was heated manually to produce an outer diameter of 100 to 200 μm.

Cell polarization model

The time-average DEP force applied on the cells can be defined as in Eq. 1 (*46*)

$$F_{\mathrm{DEP}} = 2\pi r^3 \varepsilon_{\mathrm{m}} \mathrm{Re}\,[K(\omega)] \nabla |E|^2 \quad (1)$$

where r refers to the radius of cells, ε_{m} is dielectric constant of solution, and $\nabla|E|^2$ is the gradient of electric field square. Re[$K(\omega)$] represents the real part of the Clausius-Mossotti factor, where $\omega = 2\pi f$ and f is the applied frequency by signal generator. Equation 2 is expression of $K(\omega)$

$$K(\omega) = \frac{\varepsilon_{\mathrm{p}}^* - \varepsilon_{\mathrm{m}}^*}{\varepsilon_{\mathrm{p}}^* + 2\varepsilon_{\mathrm{m}}^*} \quad (2)$$

where $\varepsilon_{\mathrm{p}}^*$ and $\varepsilon_{\mathrm{m}}^*$ are the effective complex permittivity of cell and solution, respectively. Because a cell is modeled as a single layer of shell core model, the cell contains cell membrane and cytoplasm. Then, $\varepsilon_{\mathrm{p}}^*$ can be referred to as Eq. 3

$$\varepsilon_{\mathrm{p}}^* = C_{\mathrm{mem}}\, r \frac{j\omega\tau_{\mathrm{c}} + 1}{j\omega(\tau_{\mathrm{c}} + \tau_{\mathrm{m}}) + 1} \quad (3)$$

where C_{mem} is the cell membrane capacitance, $\tau_{\mathrm{m}} = C_{\mathrm{mem}} r/\sigma_{\mathrm{c}}$, $\tau_{\mathrm{c}} = \varepsilon_{\mathrm{c}}/\sigma_{\mathrm{c}}$, and ε and σ represent dielectric constant and conductivity, respectively. The subscripts c, mem, and m represent cytoplasm, cell membrane, and solution, respectively.

According to Eq. 1, it is evident that the sign of Re[$K(\omega)$] will affect the direction of DEP force on cells. When the Re[$K(\omega)$] is equal to zero, the applied frequency is called crossover frequency (see fig. S2). When applied frequency is higher than crossover frequency, the cells are applied a positive DEP force and vice versa. By simplifying the above equations, we can conclude the relationship between cell motion and cell membrane capacitance, as shown in Eq. 4 (*47*)

$$C_{\mathrm{mem}} = \frac{\sqrt{2}\,\sigma_{\mathrm{m}}}{2\pi r f_{\mathrm{crossover}}} \quad (4)$$

Ethical approval of the study

This study was conducted according to the principles expressed in the Declaration of Helsinki. Ascites, lavage fluids, and blood were collected after obtaining informed consent from patients in accordance with institutional ethical guidelines of IRB, which were reviewed and approved by the Research Ethics Committee of China Medical University (Shenyang, China).

Clinical samples

Ascites were obtained from patients with gastric cancer treated in the First Hospital of China Medical University. Five peritoneal lavage fluids were obtained from patients with hysteromyoma who underwent abdominal surgery in Sheng Jing Hospital of China Medical University. Ascites and lavage fluids were centrifuged 10 min at 1000*g* and pelleted cells were stored in −80°C for further use. Blood samples were collected from patients with benign diseases who had no evidence of any stomach disease or other malignancy. Before storage, the cells were washed with red blood cell lysis buffer if they contained blood cells.

Cell culture, mixture, and preparation

The SGC-7901 cell line was purchased from the Institute of Biochemistry and Cell Biology at the Chinese Academy of Sciences (Shanghai,

China) and cultured at 37°C in RPMI 1640 medium (Invitrogen, USA). Cell culture medium was supplemented with 10% fetal bovine serum and incubated at 37°C with 5% CO_2.

Before mixture with lavage cells, SGC-7901 cells were fluorescently labeled with CellTracker Green CMFDA (C2925, Thermo Fisher Scientific, USA) at 37°C for 30 min in serum-free medium, washed twice with phosphate-buffered saline (PBS; Invitrogen, USA), and allowed to recover for 30 min in complete medium. Then, the cells were digested by trypsin (Invitrogen, USA) and mixed with hysteromyoma lavage cells in different ratios. In this process, we first prepared 1 million hysteromyoma lavage cells. Next, corresponding numbers of fluorescently labeled SGC-7901 cells were added and mixed well by pipette. For ratios of 1:10, 1:20, 1:50, 1:100, and 1:1000 (cancer cells:hysteromyoma lavage cells), 1×10^5, 5×10^4, 2×10^4, 1×10^4, and 1000 SGC-7901 cells were added to 1 million hysteromyoma lavage cells, respectively. For the double-stained cell mixtures, hysteromyoma lavage cells were fluorescently labeled with CellTracker Red CMPTX (C34552, Thermo Fisher Scientific, USA) for 30 min in serum-free medium and washed twice with PBS (Invitrogen, USA). Then, 1000 SGC-7901 cells were added to 500,000 hysteromyoma lavage cells. For cancer and leukocytes mixtures, 5000 SGC-7901 cells were added to 500,000 leukocytes from blood samples.

Before every experiment, the cell mixtures were centrifuged twice with a low-speed centrifuge (SC-3610, Anhui USTC Zonkia Scientific Instruments Co. Ltd., China) at 1000 RPM for 5 min. Then, the cell mixture was washed with isosmotic solution. The isosmotic solution was 0.2 M sucrose solution (V900116, Sigma-Aldrich, USA) and contained 0.59 to 0.99 weight % bovine serum albumin (V900933, Sigma-Aldrich, USA) to adjust the liquid conductivity.

Simulation for DEP force

To show the direction of positive and negative DEP force applied on the cells, we used a finite element method for numerical analysis software (Multiphysics, COMSOL AB, Sweden). The parameters used in the analysis were written as follows. The illuminated area on the a-Si:H included green color and blue color, so the conductivity was 9.6×10^{-5} S/m for green and 1.8×10^{-4} S/m for blue. The dark conductivity of the nonilluminated area was 1×10^{-11} S/m. The relative dielectric constant for a-Si:H was 11. The solution conductivity and relative dielectric constant were 1×10^{-3} S/m and 78.5, respectively. The 10 Vpp AC voltage with a frequency of 70 kHz was applied on the top and bottom ITO glass.

Wright-Giemsa staining

Cells were smeared on adhesive slides and dried at room temperature. Wright-Giemsa staining was performed using the Wright-Giemsa stain kit (BA-4017, BASO, China) according to the manufacturer's instructions. Briefly, 0.5 ml of Wright-Giemsa staining solution A was added to the slide and stained for 1 min. Then, 1 ml of solution B was added to solution A, blown with an aurilave to mix the solutions well. After 5 min, the slides were washed by distilled water, dried at room temperature, and fixed by neutral balsam. The slides were scanned by Pannoramic MIDI (3DHISTECH, Hungary).

Immunofluorescence

Cells were smeared on climbing coverslips. After washing with PBS, cells were fixed with 4% formaldehyde for 30 min. Then, cells were incubated with primary EpCAM antibody (ab71916, Abcam) at 4°C overnight. Subsequently, cells were incubated with a 1:1000 dilution of the secondary goat anti-rabbit immunoglobulin G (A-11012, Invitrogen, USA) for 1 hour and counterstained with 4′,6-diamidino-2-phenylindole for 5 min to stain cell nuclei. The slides were scanned by Leica DM6000B (Leica, Germany).

Immunohistochemistry

Peritoneal lavage fluids were spun down 20 min at 2000*g* and pelleted cells were used for immunohistochemistry. The collected cells were fixed in 4% formaldehyde and embedded in paraffin. Then, 5-μm sections of the tissue samples were deparaffinized in xylene and rehydrated through descending concentrations of ethanol. After endogenous peroxidase blockage, the sections were incubated with antibodies against MOC-31 (M3525, Dako) at 4°C overnight and then incubated with secondary antibody at room temperature for 60 min. After washing with phosphate buffered solution with Tween-20 (PBST), diluted 3,3′-diaminobenzidine was added as substrate for staining in the dark and counterstained with hematoxylin. The results were confirmed by the professional pathological doctor.

Pooled analysis of overall purity

The overall purity of the cell separation was analyzed through pooled analysis by Stata software, version 12.0 (Stata Corp, College Station, TX, USA). Briefly, we used three commands as follows: (i) gen $R = n/N$, where R is the purity of one sample, n refers to the number of cancer cells, and N is the number of total separated cells. (ii) gen ser = sqrt(R*(1 − R)/N), where ser refers to the SE of the purity. (iii) metan R ser, fixed. According to command (iii), Stata software will analyze the overall purity.

Statistical analysis

All statistical analyses in this study were performed using SPSS 20.0 software (IBM Corp, USA). Data are listed as means ± SD. Student's t test was used to analyze the difference between two groups. One-way ANOVA with Bonferroni method was used to determine the differences between cell membrane capacitances and crossover frequency among multiple groups. $P < 0.05$ from a two-tailed test was considered significant.

SUPPLEMENTARY MATERIALS

Supplementary material for this article is available at http://advances.sciencemag.org/cgi/content/full/6/32/eaba9628/DC1

View/request a protocol for this paper from *Bio-protocol*.

REFERENCES AND NOTES

1. F. Bray, J. Ferlay, I. Soerjomataram, R. L. Siegel, L. A. Torre, A. Jemal, Global cancer statistics 2018: GLOBOCAN estimates of incidence and mortality worldwide for 36 cancers in 185 countries. *CA Cancer J. Clin.* **68**, 394–424 (2018).
2. M. Ikeguchi, S. Matsumoto, S. Yoshioka, D. Murakami, S. Kanaji, S. Ohro, K. Yamaguchi, H. Saito, S. Tatebe, A. Kondo, S. Tsujitani, N. Kaibara, Laparoscopic-assisted intraperitoneal chemotherapy for patients with scirrhous gastric cancer. *Chemotherapy* **51**, 15–20 (2005).
3. T. Nishina, N. Boku, M. Gotoh, Y. Shimada, Y. Hamamoto, H. Yasui, K. Yamaguchi, H. Kawai, N. Nakayama, K. Amagai, J. Mizusawa, K. Nakamura, K. Shirao, A. Ohtsu; Gastrointestinal Oncology Study Group of the Japan Clinical Oncology, Randomized phase II study of second-line chemotherapy with the best available 5-fluorouracil regimen versus weekly administration of paclitaxel in far advanced gastric cancer with severe peritoneal metastases refractory to 5-fluorouracil-containing regimens (JCOG0407). *Gastric Cancer* **19**, 902–910 (2016).
4. Y. Yonemura, E. Bandou, T. Kawamura, Y. Endou, T. Sasaki, Quantitative prognostic indicators of peritoneal dissemination of gastric cancer. *Eur. J. Surg. Oncol.* **32**, 602–606 (2006).

5. S. Koga, N. Kaibara, Y. Iitsuka, H. Kudo, A. Kimura, H. Hiraoka, Prognostic significance of intraperitoneal free cancer cells in gastric cancer patients. *J. Cancer Res. Clin. Oncol.* **108**, 236–238 (1984).
6. E. Higaki, S. Yanagi, N. Gotohda, T. Kinoshita, T. Kuwata, M. Nagino, A. Ochiai, S. Fujii, Intraoperative peritoneal lavage cytology offers prognostic significance for gastric cancer patients with curative resection. *Cancer Sci.* **108**, 978–986 (2017).
7. M. Yanez-Mo, E. Lara-Pezzi, R. Selgas, M. Ramirez-Huesca, C. Dominguez-Jimenez, J. A. Jimenez-Heffernan, A. Aguilera, J. A. Sanchez-Tomero, M. A. Bajo, V. Alvarez, M. A. Castro, G. del Peso, A. Cirujeda, C. Gamallo, F. Sanchez-Madrid, M. Lopez-Cabrera, Peritoneal dialysis and epithelial-to-mesenchymal transition of mesothelial cells. *N. Engl. J. Med.* **348**, 403–413 (2003).
8. Y. Kodera, H. Nakanishi, S. Ito, Y. Yamamura, Y. Kanemitsu, Y. Shimizu, T. Hirai, K. Yasui, T. Kato, M. Tatematsu, Quantitative detection of disseminated free cancer cells in peritoneal washes with real-time reverse transcriptase-polymerase chain reaction: A sensitive predictor of outcome for patients with gastric carcinoma. *Ann. Surg.* **235**, 499–506 (2002).
9. S. Tsutsumi, T. Asao, T. Shimura, E. Mochiki, R. Kato, H. Kuwano, A novel rapid colorimetric assay of carcinoembryonic antigen levels in the abdominal cavity to detect peritoneal micrometastasis during gastric cancer surgery. *Cancer Lett.* **149**, 1–5 (2000).
10. S. Abe, H. Yoshimura, H. Tabara, M. Tachibana, N. Monden, T. Nakamura, S. Nagaoka, Curative resection of gastric cancer: Limitation of peritoneal lavage cytology in predicting the outcome. *J. Surg. Oncol.* **59**, 226–229 (1995).
11. S. Riethdorf, L. O'Flaherty, C. Hille, K. Pantel, Clinical applications of the CellSearch platform in cancer patients. *Adv. Drug Deliv. Rev.* **125**, 102–121 (2018).
12. G. M. Whitesides, The origins and the future of microfluidics. *Nature* **442**, 368–373 (2006).
13. C. Liu, J. Guo, F. Tian, N. Yang, F. Yan, Y. Ding, J. Wei, G. Hu, G. Nie, J. Sun, Field-free isolation of exosomes from extracellular vesicles by microfluidic viscoelastic flows. *ACS Nano* **11**, 6968–6976 (2017).
14. K. T. Kotz, W. Xiao, C. Miller-Graziano, W.-J. Qian, A. Russom, E. A. Warner, L. L. Moldawer, A. De, P. E. Bankey, B. O. Petritis, D. G. Camp II, A. E. Rosenbach, J. Goverman, S. P. Fagan, B. H. Brownstein, D. Irimia, W. Xu, J. Wilhelmy, M. N. Mindrinos, R. D. Smith, R. W. Davis, R. G. Tompkins, M. Toner; Inflammation and the Host Response to Injury Collaborative Research Program, Clinical microfluidics for neutrophil genomics and proteomics. *Nat. Med.* **16**, 1042–1047 (2010).
15. D. Di Carlo, J. F. Edd, D. Irimia, R. G. Tompkins, M. Toner, Equilibrium separation and filtration of particles using differential inertial focusing. *Anal. Chem.* **80**, 2204–2211 (2008).
16. D. D. Carlo, D. Irimia, R. G. Tompkins, M. Toner, Continuous inertial focusing, ordering, and separation of particles in microchannels. *Proc. Natl. Acad. Sci. U.S.A.* **104**, 18892–18897 (2007).
17. L. Qin, W. Zhou, S. Zhang, B. Cheng, S. Wang, S. Li, Y. Yang, S. Wang, K. Liu, N. Zhang, Highly efficient isolation of circulating tumor cells using a simple wedge-shaped microfluicdic device. *IEEE Trans. Biomed. Eng.* **66**, 1536–1541 (2018).
18. C. Xing, F. C. Da, C. L. Chang, L. Hui, Microfluidic chip for blood cell separation and collection based on crossflow filtration. *Sensors Actuators B Chem.* **130**, 216–221 (2008).
19. B. Landenberger, H. Höfemann, S. Wadle, A. Rohrbach, Microfluidic sorting of arbitrary cells with dynamic optical tweezers. *Lab Chip* **12**, 3177–3183 (2012).
20. X. Wang, S. Chen, M. Kong, Z. Wang, K. D. Costa, R. A. Li, D. Sun, Enhanced cell sorting and manipulation with combined optical tweezer and microfluidic chip technologies. *Lab Chip* **11**, 3656–3662 (2011).
21. M. M. Wang, E. Tu, D. E. Raymond, J. M. Yang, H. Zhang, N. Hagen, B. Dees, E. M. Mercer, A. H. Forster, I. Kariv, P. J. Marchand, W. F. Butler, Microfluidic sorting of mammalian cells by optical force switching. *Nat. Biotechnol.* **23**, 83–87 (2005).
22. S. B. N. Gourikutty, C.-P. Chang, P. D. Puiu, Microfluidic immunomagnetic cell separation from whole blood. *J. Chromatogr. B* **1011**, 77–88 (2015).
23. J. Nam, H. Lim, C. Kim, J. Y. Kang, S. Shin, Density-dependent separation of encapsulated cells in a microfluidic channel by using a standing surface acoustic wave. *Biomicrofluidics* **6**, 442–147 (2012).
24. X. Ding, Z. Peng, S.-C. S. Lin, M. Geri, S. Li, P. Li, Y. Chen, M. Dao, S. Suresh, T. J. Huang, Cell separation using tilted-angle standing surface acoustic waves. *Proc. Natl. Acad. Sci.* **111**, 12992 (2014).
25. M. Wu, Y. Ouyang, Z. Wang, R. Zhang, P.-H. Huang, C. Chen, H. Li, P. Li, D. Quinn, M. Dao, S. Suresh, Y. Sadovsky, T. J. Huang, Isolation of exosomes from whole blood by integrating acoustics and microfluidics. *Proc. Natl. Acad. Sci. U.S.A.* **114**, 10584–10589 (2017).
26. Z. Wang, F. Li, J. Rufo, C. Chen, S. Yang, L. Li, J. Zhang, J. Cheng, Y. Kim, M. Wu, E. Abemayor, M. Tu, D. Chia, R. Spruce, N. Batis, H. Mehanna, D. T. W. Wong, T. J. Huang, Acoustofluidic salivary exosome isolation: A liquid biopsy compatible approach for human papillomavirus–associated oropharyngeal cancer detection. *J. Mol. Diagn.* **22**, 50–59 (2020).
27. M. Wu, C. Chen, Z. Wang, H. Bachman, Y. Ouyang, P.-H. Huang, Y. Sadovsky, T. J. Huang, Separating extracellular vesicles and lipoproteins via acoustofluidics. *Lab Chip* **19**, 1174–1182 (2019).
28. S. Sangjo, S. H. Katherine, N. Jamileh, F. F. Becker, P. R. C. Gascoyne, Dielectrophoresis has broad applicability to marker-free isolation of tumor cells from blood by microfluidic systems. *Biomicrofluidics* **7**, 011808 (2013).
29. H. S. Moon, K. Kwon, S. I. Kim, H. Han, J. Sohn, S. Lee, H. I. Jung, Continuous separation of breast cancer cells from blood samples using multi-orifice flow fractionation (MOFF) and dielectrophoresis (DEP). *Lab Chip* **11**, 1118–1125 (2011).
30. S. Park, Y. Zhang, T.-H. Wang, S. Yang, Continuous dielectrophoretic bacterial separation and concentration from physiological media of high conductivity. *Lab Chip* **11**, 2893–2900 (2011).
31. M. Antfolk, S. H. Kim, S. Koizumi, T. Fujii, T. Laurell, Label-free single-cell separation and imaging of cancer cells using an integrated microfluidic system. *Sci. Rep.* **7**, 46507 (2017).
32. P. Y. Chiou, A. T. Ohta, M. C. Wu, Massively parallel manipulation of single cells and microparticles using optical images. *Nature* **436**, 370–372 (2005).
33. H. Song-Bin, L. Shing-Lun, L. Jian-Ting, W. Min-Hsien, Label-free live and dead cell separation method using a high-efficiency optically-induced dielectrophoretic (ODEP) force-based microfluidic platform. *Int. J. Autom. Smart Technol.* **4**, 83–91 (2014).
34. W. Liang, Y. Zhao, L. Liu, Y. Wang, Z. Dong, W. J. Li, G.-B. Lee, X. Xiao, W. Zhang, Rapid and label-free separation of Burkitt's lymphoma cells from red blood cells by optically-induced electrokinetics. *PLOS ONE* **9**, e90827 (2014).
35. Y.-H. Lin, Y.-W. Yang, Y.-D. Chen, S.-S. Wang, Y.-H. Chang, M.-H. Wu, The application of an optically switched dielectrophoretic (ODEP) force for the manipulation and assembly of cell-encapsulating alginate microbeads in a microfluidic perfusion cell culture system for bottom-up tissue engineering. *Lab Chip* **12**, 1164–1173 (2012).
36. T.-K. Chiu, A.-C. Chao, W.-P. Chou, C.-J. Liao, H.-M. Wang, J.-H. Chang, P.-H. Chen, M.-H. Wu, Optically-induced-dielectrophoresis (ODEP)-based cell manipulation in a microfluidic system for high-purity isolation of integral circulating tumor cell (CTC) clusters based on their size characteristics. *Sensors Actuators B Chem.* **258**, 1161–1173 (2018).
37. T.-K. Chiu, W.-P. Chou, S.-B. Huang, H.-M. Wang, Y.-C. Lin, C.-H. Hsieh, M.-H. Wu, Application of optically-induced-dielectrophoresis in microfluidic system for purification of circulating tumour cells for gene expression analysis—Cancer cell line model. *Sci. Rep.* **6**, 32851 (2016).
38. S.-B. Huang, M.-H. Wu, Y.-H. Lin, C.-H. Hsieh, C.-L. Yang, H.-C. Lin, C.-P. Tseng, G.-B. Lee, High-purity and label-free isolation of circulating tumor cells (CTCs) in a microfluidic platform by using optically-induced-dielectrophoretic (ODEP) force. *Lab Chip* **13**, 1371–1383 (2013).
39. H. Nakanishi, Y. Kodera, Y. Yamamura, S. Ito, T. Kato, T. Ezaki, M. Tatematsu, Rapid quantitative detection of carcinoembryonic antigen-expressing free tumor cells in the peritoneal cavity of gastric-cancer patients with real-time RT-PCR on the lightcycler. *Int. J. Cancer* **89**, 411–417 (2000).
40. J. P. De Andrade, J. J. Mezhir, The critical role of peritoneal cytology in the staging of gastric cancer: An evidence-based review. *J. Surg. Oncol.* **110**, 291–297 (2014).
41. A. Seeber, A. Martowicz, G. Spizzo, T. Buratti, P. Obrist, D. Fong, G. Gastl, G. Untergasser, Soluble EpCAM levels in ascites correlate with positive cytology and neutralize catumaxomab activity in vitro. *BMC Cancer* **15**, 372 (2015).
42. C. E. Morris, U. Homann, Cell surface area regulation and membrane tension. *J. Membr. Biol.* **179**, 79–102 (2001).
43. P. R. C. Gascoyne, S. Shim, J. Noshari, F. F. Becker, K. Stemke-Hale, Correlations between the dielectric properties and exterior morphology of cells revealed by dielectrophoretic field-flow fractionation. *Electrophoresis* **34**, 1042–1050 (2013).
44. Y. Huang, X. B. Wang, P. R. C. Gascoyne, F. F. Becker, Membrane dielectric responses of human T-lymphocytes following mitogenic stimulation. *Biochim. Biophys. Acta* **1417**, 51–62 (1999).
45. X. B. Wang, Y. Huang, P. R. C. Gascoyne, F. F. Becker, R. Pethig, Changes in friend murine erythroleukaemia cell membranes during induced differentiation determined by electrorotation. *Biochim. Biophys. Acta* **1193**, 330–344 (1994).
46. T. B. Jones, *Electromechanics of Particles: Fundamentals* (Cambridge Univ. Press, 1995).
47. P. Ronald, Review article-dielectrophoresis: status of the theory, technology, and applications. *Biomicrofluidics* **4**, 39901 (2010).

Acknowledgments

Funding: We wish to acknowledge the funding provided by the National Natural Science Foundation of China (project nos. 61925307, U1908207, 61727811, 91748212, and 61973224), the National Key R&D Program of China (project nos. 2018YFB1304900 and 2017YFC0908300), the Joint Project in Key Area of Liaoning Province Natural Science Foundation (project no. 2019-KF-01-10), the Youth Innovation Promotion Association CAS (project no. Y201943), and the Hong Kong Research Grants Council's Joint Laboratory Funding Scheme (project no. JLFS/E-104/18). **Author contributions:** W.J.L., Z.W., L.L., and H.Y. supervised the project. W.J.L., Z.W., and L.L. designed experiments. H.Y., Y.Z., and J.Z. performed experiments. Y.Z. fabricated

the OEK-based microfluidic chip and analyzed cell membrane capacitance data. Z.W. and J.Z. provided clinical samples, cytological examinations, and the pooled analysis. P.L. and W.L. helped to design and analyze the OEK-based data. Z.L. helped to design the OEK system. G.-B.L. provided the OEK chips. Y.Z. and J.Z. wrote the manuscript with input from all the authors. **Competing interests:** The authors declare that they have no competing interests. **Data and materials availability:** All data needed to evaluate the conclusions in the paper are present in the paper and/or the Supplementary Materials. Additional data related to this paper may be requested from authors.

Submitted 19 January 2020
Accepted 22 June 2020
Published 5 August 2020
10.1126/sciadv.aba9628

Citation: Y. Zhang, J. Zhao, H. Yu, P. Li, W. Liang, Z. Liu, G.-B. Lee, L. Liu, W. J. Li, Z. Wang, Detection and isolation of free cancer cells from ascites and peritoneal lavages using optically induced electrokinetics (OEK). *Sci. Adv.* **6**, eaba9628 (2020).